

RESEARCH ARTICLE | MAY 03 2023

Ordinal pattern-based complexity analysis of high-dimensional chaotic time series

Special Collection: [Nonlinear dynamics, synchronization and networks: Dedicated to Jürgen Kurths' 70th birthday](#)

Inga Kottlarz ; Ulrich Parlitz ✉



Chaos 33, 053105 (2023)

<https://doi.org/10.1063/5.0147219>



View
Online



Export
Citation

CrossMark

Articles You May Be Interested In

Ordinal methods for a characterization of evolving functional brain networks

Chaos (February 2023)

Continuous ordinal patterns: Creating a bridge between ordinal analysis and deep learning

Chaos (March 2023)

Ordinal response model of community response

J Acoust Soc Am (September 2015)



Chaos

Special Topic: Nonlinear Model Reduction From Equations and Data

Submit Today!

Ordinal pattern-based complexity analysis of high-dimensional chaotic time series

Cite as: Chaos 33, 053105 (2023); doi: 10.1063/5.0147219

Submitted: 20 February 2023 · Accepted: 4 April 2023 ·

Published Online: 3 May 2023





View Online



Export Citation



CrossMark

Inga Kottlarz^{1,2,3,4,a)}  and Ulrich Parlitz^{1,2,4,b)} 

AFFILIATIONS

¹Max Planck Institute for Dynamics and Self-Organization, Am Fassberg 17, 37077 Göttingen, Germany

²Institute for the Dynamics of Complex Systems, Georg-August-Universität Göttingen, Friedrich-Hund-Platz 1, 37077 Göttingen, Germany

³Department of Pharmacology and Toxicology, University Medical Center Göttingen (UMG), Robert-Koch-Str. 40, 37075 Göttingen, Germany

⁴German Center for Cardiovascular Research (DZHK), partner site Göttingen, Robert-Koch-Str. 42a, 37075 Göttingen, Germany

Note: This paper is part of the Focus Issue on Nonlinear dynamics, synchronization and networks: Dedicated to Juergen Kurths' 70th birthday.

^{a)}inga.kottlarz@ds.mpg.de

^{b)}**Author to whom correspondence should be addressed:** ulrich.parlitz@ds.mpg.de

ABSTRACT

The ordinal pattern-based complexity–entropy plane is a popular tool in nonlinear dynamics for distinguishing stochastic signals (noise) from deterministic chaos. Its performance, however, has mainly been demonstrated for time series from low-dimensional discrete or continuous dynamical systems. In order to evaluate the usefulness and power of the complexity–entropy (CE) plane approach for data representing high-dimensional chaotic dynamics, we applied this method to time series generated by the Lorenz-96 system, the generalized Hénon map, the Mackey–Glass equation, the Kuramoto–Sivashinsky equation, and to phase-randomized surrogates of these data. We find that both the high-dimensional deterministic time series and the stochastic surrogate data may be located in the same region of the complexity–entropy plane, and their representations show very similar behavior with varying lag and pattern lengths. Therefore, the classification of these data by means of their position in the CE plane can be challenging or even misleading, while surrogate data tests based on (entropy, complexity) yield significant results in most cases.

© 2023 Author(s). All article content, except where otherwise noted, is licensed under a Creative Commons Attribution (CC BY) license (<http://creativecommons.org/licenses/by/4.0/>). <https://doi.org/10.1063/5.0147219>

The complexity–entropy (CE) plane is a popular tool in time series analysis for the separation of stochastic and chaotic processes. It is based on the concept of ordinal patterns, an approach to mapping a real-valued time series into a symbolic sequence whose statistical properties can be quantified in terms of entropies and complexity measures. We investigate the usability of the CE plane for the analysis of time series generated by different types of high-dimensional dynamical systems and find that there are data from random processes that exhibit the same behavior in the CE plane that was originally thought to be characteristic of high-dimensional chaos.

I. INTRODUCTION

The term “complexity” is one that is widely used across many fields, and there are many definitions of it. In dynamical systems theory, “complexity” is usually associated with a system that displays chaotic behavior, in contrast to periodic or stochastic systems. The characterization of such systems, and the distinction from purely (“boring”) random behavior, has been a subject of study for a long time now. Many (often very similar) approaches have been suggested to classifying a time series from an unknown origin as either “complex” or random.^{1–8}

A straightforward approach to characterizing the complexity of a time series has been dynamical entropies.³ Their disadvantage is, however, that they are large both for chaotic systems and purely random ones, rendering them incapable of differentiating between the two.^{1,4} This has inspired several authors to find an alternative or additional measure to better distinguish noise from chaos. The method investigated in this work is the *complexity–entropy plane* (CE plane, sometimes also referred to as complexity–entropy–causality plane) introduced by Rosso *et al.*⁴ It is based on *ordinal pattern statistics*,³ an approach to the symbolization of time series. In addition to the widely used *permutation entropy*, it uses a second quantity, the so-called *statistical complexity* of a time series for characterization of data.

The statistical complexity is defined by Rosso *et al.*⁴ via the Jensen–Shannon divergence of a distribution of symbols (patterns) to a uniform distribution. This way, a time series with maximum entropy has zero complexity. To ensure that regular data (with a non-uniform distribution of patterns and a low entropy) also display low complexity, the Jensen–Shannon divergence is multiplied with the permutation entropy value. This results in two dependent quantities, the entropy and the complexity, that both compare a distribution of patterns to a uniform distribution. The *permutation entropy* and the *statistical complexity* of a time series, i.e., its position in the CE plane, are widely used to characterize the complexity (or chaoticity) of time series or to distinguish between data of different origins.^{10–18}

While several studies have examined the separation of stochastic time series and low-dimensional discrete chaotic dynamical systems in the complexity–entropy (CE) plane, the analysis of data from dynamical systems exhibiting high-dimensional chaos has been somewhat neglected. An exception is a study of Zunino *et al.*¹² who investigated high-dimensional time series generated by the Mackey–Glass equation¹⁹ and found that the estimated complexity values highly depend on the lag of the ordinal patterns used. In this work, we aim to investigate the influence of increasing dimension of the attractor underlying the analyzed time series on estimated complexity and entropy values and to develop a guide on how to analyze (possibly very high-dimensional) real-world time series using the CE plane.

To do so, we chose high-dimensional dynamical systems from four different categories, representing continuous, discrete, time delay, and spatiotemporal chaos. For each system, we varied the attractor dimension, here estimated by the Kaplan–Yorke dimension. We compared the position of phase randomized surrogates in the CE plane with that of the original hyperchaotic time series and found that a visual distinction between the two is often barely possible, even in cases where a surrogate data test yields significant results. Even more important for the interpretation of the CE-diagrams, however, is the fact that stochastic surrogate data and time series from deterministic systems occur close together in the same region of the CE plane. This suggests that the more popular practice of visual distinction via the position on the CE plane can be problematic.

II. DYNAMICAL SYSTEMS

We chose four different high-dimensional dynamical systems for our comparison: the Lorenz-96 system²⁰ as a continuous

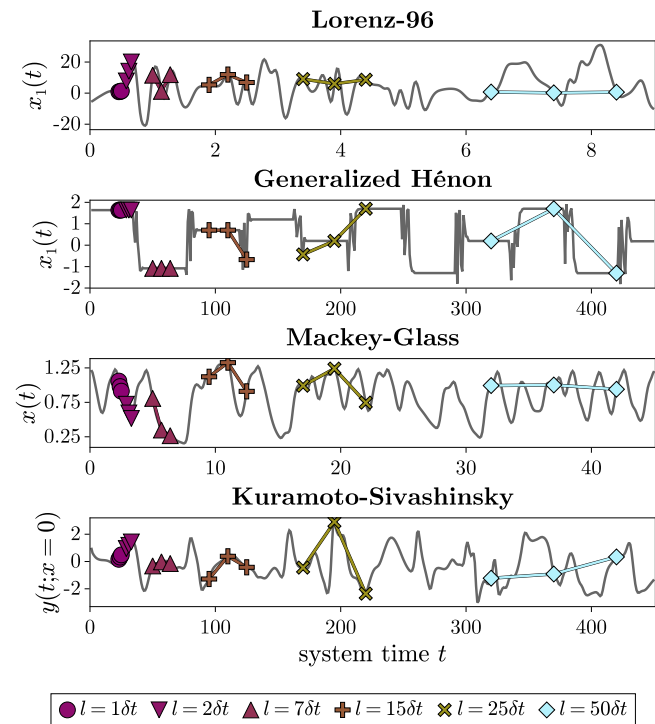


FIG. 1. Patterns of different lags in original time series with $\Delta^{(KY)} \approx 43$ (corresponding values for D , τ , L are given in Table I). The time series for the Lorenz-96 system, the generalized Hénon map, and the Kuramoto–Sivashinsky equation are from one individual variable or spatial measurement point in the case of the Kuramoto–Sivashinsky equation.

system, the discrete generalized Hénon map,^{21–23} the Mackey–Glass equation¹⁹ as an example of a time-delay system, and the spatiotemporally chaotic Kuramoto–Sivashinsky equation.^{24,25} The dynamical rule of each system is given in the following. The sampling times δt of the continuous-time systems were adjusted such that a given number of samples shows approximately the same number of oscillations for comparability; see also exemplary plots of time series in Fig. 1. The sampling rates δt , as well as all other parameters necessary to reproduce the simulations, are given in Table I.

a. *The Lorenz-96 system*²⁰ is a continuous-time dynamical system that can be simulated for an arbitrary number of dimensions $D \geq 4$. It is defined by

$$\dot{x}_i = (x_{i+1} - x_{i-2})x_{i-1} - x_i + F, \quad i = 1, 2, \dots, D. \quad (1)$$

The dynamical elements are grouped together as a ring such that $x_{-1} \equiv x_{D-1}$, $x_0 \equiv x_D$, and $x_{D+1} \equiv x_1$. For the purpose of this work, the constant forcing is set to $F = 24$. Due to the structure of the equation, the Lorenz-96 system can also be considered a one-dimensional spatiotemporal system with periodic boundary conditions.

b. *The generalized Hénon map*^{21–23} is a discrete-time dynamical system and can be implemented for an arbitrary number of dimensions $D \geq 2$. In this work, the definition by Baier and Klein²¹ is used

TABLE I. Integration parameters of investigated systems. We refer to the sampling time step as δt and to the integration time step as Δt . The *dimensionality* column gives the range of the parameter, which determines the Kaplan–Yorke dimension. In all cases, $\Delta^{(KY)}$ ranges between approximately 3 and 50.

System	Initial condition	Parameters	Integration	Dimensionality
Lorenz-96	$x_j(0) = j \cdot 0.1$ for $j = 0, \dots, D - 1$	$F = 24$	Tsit5 ⁹ adaptive time step, $\delta t = 0.02$	$D = \{4, 5, 6, \dots, 50\}$, $\Delta^{(KY)} \approx 43$ for $D = 50$
Generalized Hénon Mackey–Glass	$x_i(0) = 0 \forall i$ $x(0) = 1.0$, $x(t) = 0$ for $t < 0$	$a = 1.76, b = 0.1$ $\beta = 2, \gamma = 1, \nu = 9.65$... RK4, $\Delta t = 0.1$, $\delta t = 0.2$	$D = \{2, 3, 4, \dots, 50\}$, $\Delta^{(KY)} \approx 43$ for $D = 44$ $\tau = \{2, 3, 4, \dots, 50\}$, $\Delta^{(KY)} \approx 43$ for $\tau = 39$
Kuramoto–Sivashinsky	$y(t=0, x) = \cos(x) + 0.1 \sin(x/8) + 0.01 \cos(2\pi x/L)$...	Tsit5 ⁹ in spectral domain, adaptive time step, $\Delta x = 0.2$, $\delta t = 1$	$L = \{4, 5, 6, \dots, 38\}$, $\Delta^{(KY)} \approx 43$ for $L = 30$

such that the i th variable at time step $n + 1$, $x_i(n + 1)$ is given by

$$x_i(n + 1) = a - (x_{D-1}(n))^2 - b x_D(n), \quad (2)$$

$$x_i(n + 1) = x_{i-1}(n) \quad \text{for } i = 2, \dots, D. \quad (3)$$

This map has $D - 1$ positive Lyapunov exponents for D dimensions, as is also displayed in Fig. 2.

c. The Mackey–Glass equation was introduced by Mackey and Glass^{19,26} and is a delay-differential equation that models physiological control systems. It can, depending on the time delay τ , display high-dimensional chaos.²⁷ The equation is given by

$$\dot{x}(t) = \beta \frac{x(t - \tau)}{1 + x(t - \tau)^\nu} - \gamma x(t), \quad (4)$$

with $\beta, \gamma, \nu \in \mathbb{R}_{>0}$.

d. The Kuramoto–Sivashinsky equation^{25,28} describes a one-dimensional spatiotemporal system, where

$$\partial_t y = -\partial_x^2 y - \partial_x^4 y - \frac{1}{2}(\partial_x y)^2. \quad (5)$$

For the purpose of this work, it is simulated with periodic boundary conditions on different domain sizes L .

Each of the systems is capable of displaying high-dimensional chaos. We calculated the Lyapunov spectrum of each system to estimate the Kaplan–Yorke (KY) dimension²⁸ $\Delta^{(KY)}$. The KY dimension and the Lyapunov spectra are displayed in Fig. 2. The simulations and calculation of the KY dimension were performed in Julia using the DynamicalSystems.jl²⁹ library.

A. The surrogate data approach

To address the question whether (high-dimensional) chaotic time series can be distinguished from stochastic data by their position in the CE plane, we are interested in the most challenging cases, i.e., in time series that are random but share as many features as possible with the given observable from the deterministic system. Such

stochastic time series are often called *surrogate data*, and there are many ways to generate them.³⁰

The method of surrogate data was introduced by Theiler *et al.*³¹ in 1992 as a statistical approach for identifying nonlinearities in time series, based on the widely known and applied *bootstrapping* method.³² It is a way of generating new “surrogate” time series from original (measured) data to test a specific null hypothesis.³⁰

Surrogate data are often generated by phase randomization. The original time series is transformed into Fourier space, where the phases of the spectrum are randomized. This keeps the power spectral density, and, thus, also the autocorrelation, unchanged.^{33,34} The spectrum with the randomized phases is then transformed back, which results in a time series that has the same autocorrelation as the original data, but could have been generated by a linear Gaussian process. This type of surrogates is usually referred to as *FT surrogates*.³⁰

In addition to FT surrogates, we used surrogates generated by an *amplitude adjusted Fourier transform*³¹ (AAFT surrogates). Here, the amplitude distribution is rescaled to resemble a Gaussian distribution before randomizing the phases. After phase randomization, the amplitude distribution is rescaled again to match that of the original time series.

Once the surrogate time series have been generated, a discriminatory quantity of choice can be applied. It is calculated for both original and surrogate data. If the values of the original data differ significantly from those of the surrogates in a statistical test, the null hypothesis is rejected. Assuming Gaussian distributed surrogates, this test can be as simple as calculating the standard deviation of the surrogate distribution and rejecting the null hypothesis if the original data differ several standard deviations from the mean of the surrogates.

Here, all pairwise distances between the surrogates on the CE plane are calculated to generate a distribution. A second distribution is estimated from the distances between the original data point to each surrogate. The significance is then calculated using a two-sample Kolmogorov–Smirnov test³⁵ in order to not

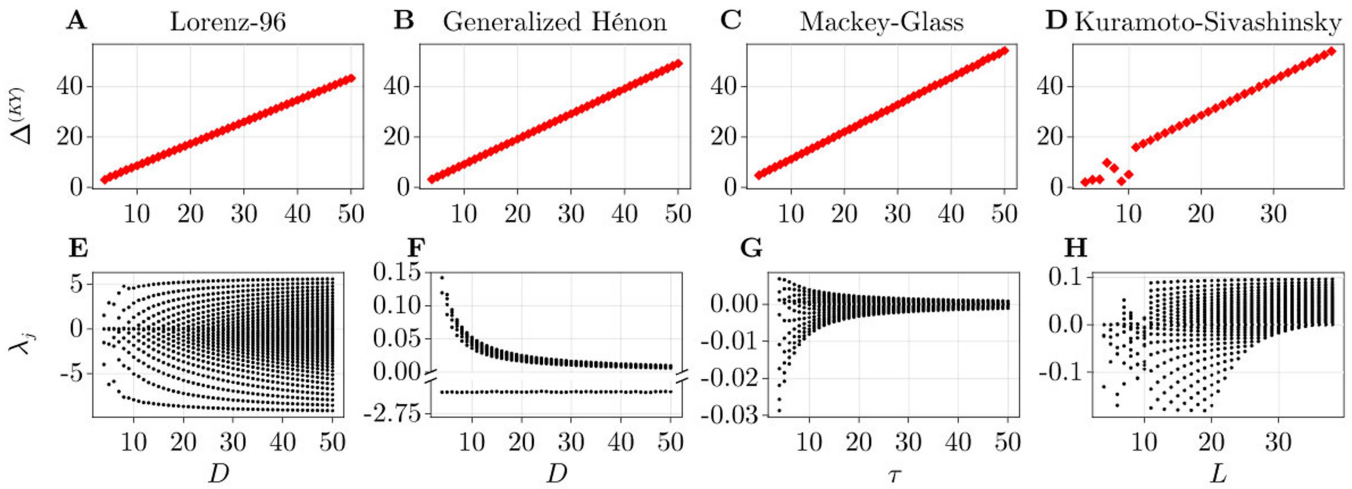


FIG. 2. Kaplan–Yorke dimension $\Delta^{(KY)}$ and the (largest) Lyapunov exponents for different dimensionalities D of (a) and (e) the Lorenz-96 system, (b) and (f) the generalized Hénon map, (c) and (g) the Mackey–Glass equation, and (d) and (h) the Kuramoto–Sivashinsky equation. System parameters are listed in Table I. For small values of the domain size L , periodic and low-dimensional chaotic attractors occur.

depend on any underlying assumptions about the distribution of surrogates.

III. THE COMPLEXITY-ENTROPY PLANE

The concept of ordinal patterns was introduced by Bandt and Pompe³ in 2002 and can be considered a subbranch of symbolic dynamics.³⁶ Originally introduced to measure complexity in time series, ordinal pattern-based methods have, for example, been successfully used to classify physiological time series,^{17,37–44} quantifying complex networks and synchronization,^{45–47} and finding similarities between neuronal and optical (laser) spikes.^{48–51} All complexity–entropy values in this paper were calculated using the open-source library ComplexityMeasures.jl.⁵²

A. Ordinal patterns and permutation entropy

In ordinal pattern analysis, a real-valued time series $x_t \in \mathbb{R}$, where $t = n\delta t$ with $n \in \mathbb{N}$ and δt being the sampling time, is transformed into a sequence of symbols from a finite alphabet. Given a length m and a lag $l = j\delta t$, $j \in \mathbb{N}$, a pattern is defined by the sample points $x_t, x_{t+l}, \dots, x_{(m-1)(t+l)}$. For a specific length m , there are $m!$ different possible patterns. Each pattern is assigned a unique *permutation index* π . If the pattern contains two identical amplitudes, these amplitudes are ordered with respect to their occurrence in time in the original formulation in Ref. 3. However, this can lead to false conclusions,⁵⁸ which is why here, one of the two values is randomly chosen to be the “larger” value.

Once a time series is translated into a sequence of symbols, this sequence can be statistically analyzed: The probabilities of occurrence of each pattern can be estimated from the series, and the Shannon entropy⁵³ $S[P]$ of that probability distribution P can be calculated.

This approach was introduced by Bandt and Pompe³ as the *permutation entropy* (PE) of the given time series.⁵⁴ It is often normalized with respect to the entropy of a uniform distribution with $m!$ bins. We define the normalized PE as

$$H_S = \frac{S[P]}{S_{\max}} = \frac{\sum_j p_j \log p_j}{\log(m!)}. \quad (6)$$

For a signal generated by a deterministic dynamical system, only some of the possible patterns of a given length m occur if one chooses a large enough pattern length. Patterns that cannot occur due to the underlying deterministic dynamical rule are called *forbidden patterns*. This results in a non-uniform distribution of patterns and, thus, a lower entropy than a more “complex” signal, where almost all patterns occur with similar probability.

It must be noted, though, that the interpretation of the word “complexity” needs to be thought of very carefully. In a (finite) time series containing only white noise, all possible patterns will occur with (almost) the same probability, resulting in the highest possible entropy—that of the uniform distribution. Thus, a more unbiased interpretation of the PE would be that it quantifies the irregularity of a signal.

On the other hand, a highly complex time series, containing not (only) white noise but an underlying deterministic complex dynamics, can also, for (too) short patterns, have a uniform distribution of patterns, thus giving the same entropy as a solely stochastic time series.

To distinguish stochastic and deterministic (chaotic) time series with non-uniform distributions, Rosso *et al.* suggested a second quantity, the *statistical complexity*,⁴ and generalized it later on.⁵⁵ In this work, only the original formulation is considered. The statistical complexity $C_{JS}[P]$ of a time series with an ordinal distribution P is defined as

$$C_{JS}[P] = H_S \cdot Q_{JS}[P, P_e]. \quad (7)$$

Here, H_S is the normalized permutation entropy as defined in Eq. (6), and Q_{JS} is the normalized Jensen–Shannon divergence between the ordinal distribution P and a uniform distribution P_e with $m!$ bins, where

$$Q_{JS}[P, P_e] = \frac{D_{JS}[P, P_e]}{D_{JS, \max}}. \quad (8)$$

The Jensen–Shannon divergence D_{JS} is calculated from the Shannon entropy S as

$$D_{JS} = S \left[\frac{P + P_e}{2} \right] - \frac{S[P]}{2} - \frac{S[P_e]}{2}. \quad (9)$$

The two quantities C_{JS} and H_S are usually used in combination with one another. Together, they span the *complexity–entropy plane* (CE plane). For a distribution with a given permutation entropy H_S , there is a minimum and maximum possible value for the complexity C_{JS} . These so-called *minimum* and *maximum complexity–entropy curves* $P \mapsto (H_S[P], C_{JS}[P, P_e])$ can be calculated according to Martin *et al.*⁵⁶

It is important to note that the above considerations are not directly applicable to continuous-time dynamical systems because the lag $l = j \delta t$ can become very small with respect to the typical time scales of the time series if the sampling time δt is (very) small. A chaotic, oversampled time series can still display comparatively low normalized permutation entropy and high complexity due to the fact that some patterns are (extremely) unlikely to occur simply because they would violate the smoothness of the curve.⁵⁷

IV. STATISTICAL COMPLEXITY OF HIGH-DIMENSIONAL DYNAMICAL SYSTEMS

While the separation of stochastic and deterministic time series in the complexity–entropy (CE) plane has been investigated by many authors for data from low-dimensional and often discrete dynamical systems,^{10,11,13–16} only very few studies for high-dimensional systems exist.¹²

The first problem to consider here is the general problem of the amount of available data: Eckmann and Ruelle⁵⁸ argued that for a faithful estimation of the Lyapunov exponents of a dynamical system with attractor dimensionality Δ , $N > 10^\Delta$ data points are required. While to our knowledge no such estimation exists for the permutation entropy of a system, one could use this estimate as an orientation for the needed amount of data for ordinal pattern-based quantities. For a time series consisting of $N \approx 10^4$ points, for example, this limits the resolvable attractor dimension to $\Delta \approx 4$. Not to mention a number of other conservative estimates for the required number of data points.^{59–61}

Viewing ordinal patterns from the delay embedding^{62–64} point of view, where classically, the embedding dimension d should be $d \geq 2\Delta$ with the attractor dimension Δ , there arises a second computational problem. If the embedding dimension in delay embedding would be equivalent to the pattern length m , one would need very large m to resolve high-dimensional systems, for example, $m = 8$, even for just a four-dimensional attractor. While this case would technically be covered by the rule of Eckmann and Ruelle, the estimation of a histogram with $8! \approx 4 \cdot 10^4$ bins cannot be done faithfully from 10^4 data points, only. Additionally, the resulting histogram would differ from a uniform distribution due to the

inevitable empty bins by construction, leading to possibly spuriously low entropy and high statistical complexity.

All of these considerations raise the question of whether analyses with ordinal pattern-based quantities provide the expected results even for data from high-dimensional dynamical systems. Zunino *et al.*¹² have done an investigation of the CE plane for high-dimensional data using the Mackey–Glass equation^{19,26} and found that the estimated complexity values highly depend on the lag of the ordinal patterns used. In this work, we confirm this result for data from different dynamical systems as well as stochastic time series obtained via phase randomization (FT and AAFT surrogates). Furthermore, we investigate the influence of increasing attractor dimension on estimated complexity and entropy values and demonstrate the potential and limitations of CE-plane analysis of (possibly very high-dimensional) real-world time series.

To investigate these issues in more detail, we studied the influence of parameters that can be chosen during the analysis, such as the pattern length and the lag used for sampling the patterns and others that are given (and unknown), such as the dimensionality of the process generating the data or the amount of data available.

A. Control parameters: Pattern length and lag

The pattern length m and the lag l used for sampling and composing the pattern can be chosen by the user performing the time series analysis and both have a major impact on the results obtained. If the pattern length m is too small, the patterns obtained cannot encode the dynamics similar to a too low embedding dimension. Therefore, the ordinal pattern distributions are (almost) uniform, resulting in high entropy and low complexity values, even in cases with a clear deterministic structure.⁶⁵ If, on the other hand, m is chosen very large, the given length of the time series is not sufficient anymore to fill all $m!$ bins, and there is a systematic bias in the opposite direction where distributions appear more non-uniform than the true distribution for this given m and l . Therefore, there is a threshold m_{\min} that has to be exceeded by the pattern length m to unfold a relevant structure in the data and another, m_{\max} , which must not be exceeded to guarantee a sound estimation of the distribution (for a given length of the time series). As long as $m_{\min} < m_{\max}$, any choice of $m \in [m_{\min}, m_{\max}]$ should provide useful ordinal pattern distributions, but for data from high dimensional systems, this may become a major challenge because there m_{\min} can be larger than m_{\max} .

Figure 3 shows the dependency of the complexity–entropy values on the pattern length m for a fixed lag l for the original time series of the systems investigated and for their FT and AAFT surrogate data. As expected, for the small values of m shown there, the entropy decreases and the complexity increases with the length m . No minimum- and maximum complexity–entropy curves are plotted in this diagram because these curves depend on the pattern length. For the continuous-time systems, we fixed the lag to the same value, but still, we find different behavior: While for the Lorenz-96 system, a clear separation between original data and surrogates is visible, this does not happen for the Mackey–Glass system. It should be noted that one can tune the parameters (lag) in a way that data from the Mackey–Glass system show the same behavior as the time

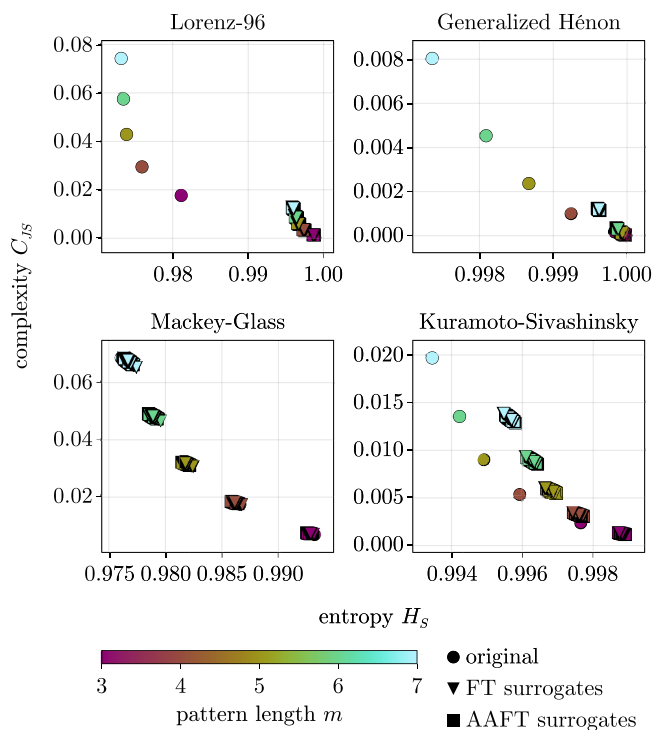


FIG. 3. Complexity–entropy values for patterns of different pattern lengths. Time series of lengths 10^6 points were considered obtained from attractors with dimensions $\Delta^{(KY)} \approx 43$ (corresponding values for D , τ , and L are given in Table I). The lags were fixed to $l = 10\delta t$ for the continuous-time systems and $l = 1$ for the generalized Hénon map.

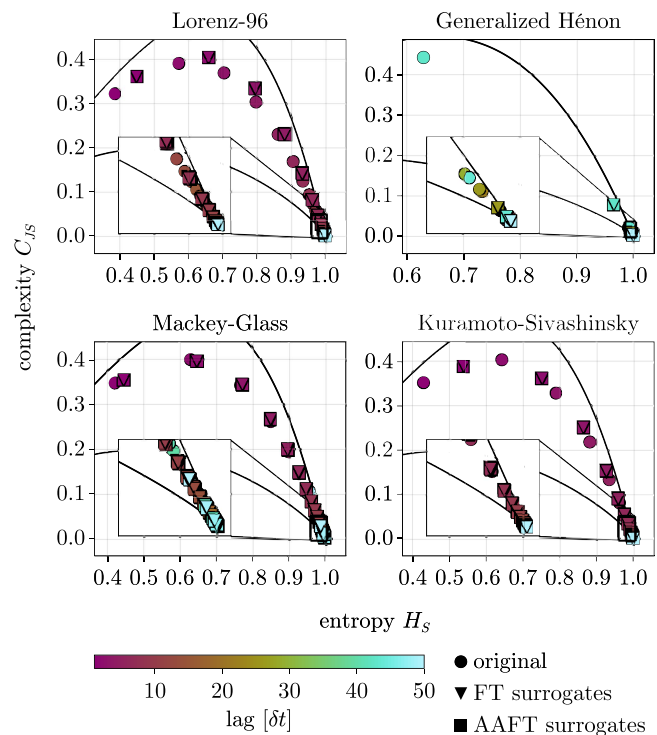


FIG. 4. Complexity–entropy values for patterns with different lags. 10^6 points were considered for systems of $\Delta^{(KY)} \approx 43$ (corresponding values for D , τ , and L are given in Table I). The pattern length was fixed to $m = 6$. The solid black lines indicate the minimum and maximum possible complexity values for given entropy.

series of the Lorenz-96 system, but we found it also noteworthy that for similar time scales, the two data sets display very different results.

In fact, the lag l is the other relevant control parameter, which has a major influence on the estimates of entropy and complexity. Large lags result in patterns, which are composed of samples far apart in time, which are (almost) statistically independent. Therefore, the resulting ordinal pattern distributions are (almost) uniform with (almost) maximum permutation entropy and vanishing complexity. For densely sampled smooth time series from continuous-time systems, another pitfall exists. For small lags l , a few patterns, such as increasing or decreasing time series values, occur with a (very) high probability due to correlations on short time scales. The corresponding very non-uniform distributions result in low or medium entropies and medium or high complexity. If the lag is increased, the complexity reaches a maximum before it decreases to zero for very large l . This characteristic dependency was first reported by Zunino *et al.*¹² for the Mackey–Glass system and is shown in Fig. 4 for the systems investigated in this study. It is important to note that for the values of the highest complexity, original and surrogate data can lie close together and follow a similar path when the lag is increased, suggesting that the intermediate entropy and high complexity values stem from fine sampling and the resulting

smoothness of the time series in combination with relatively small lags.

Interestingly, the CE values of the FT surrogates and the AAFT surrogates do not differ significantly. We conjecture that this agreement is due to the fact that ordinal patterns are invariant with respect to monotonously increasing transformations of the data, and thus, the amplitude adjustment of the AAFT method has no major impact on the results (see the Appendix).

In order to evaluate the combined impact of pattern length m and lag l , Fig. 5 shows the significance of an AAFT-surrogate data test depending on (m, l) . It can be seen that there is no common dependency of the significance on lag and word length across different dynamical systems. While the distinction tends to be more prominent for Mackey–Glass and Kuramoto–Sivashinsky systems with larger pattern lengths, time series of the Lorenz-96 system are always distinguishable from their surrogates for large amounts of data (10^6 data points). The generalized Hénon map displays a dependency mostly on the chosen lag and not so much for the pattern length. This is presumably a result of the “cyclic” structure of the map. We find that the significance is high specifically for the cases where $l = D$, and in fact, there are only a few cases for very short data lengths (10^3) (not shown here), in which significance is not given for $l = D$ for any chosen pattern length between 3 and 7. To be able to use patterns up to length $m = 7$, of course, one needs to be able to

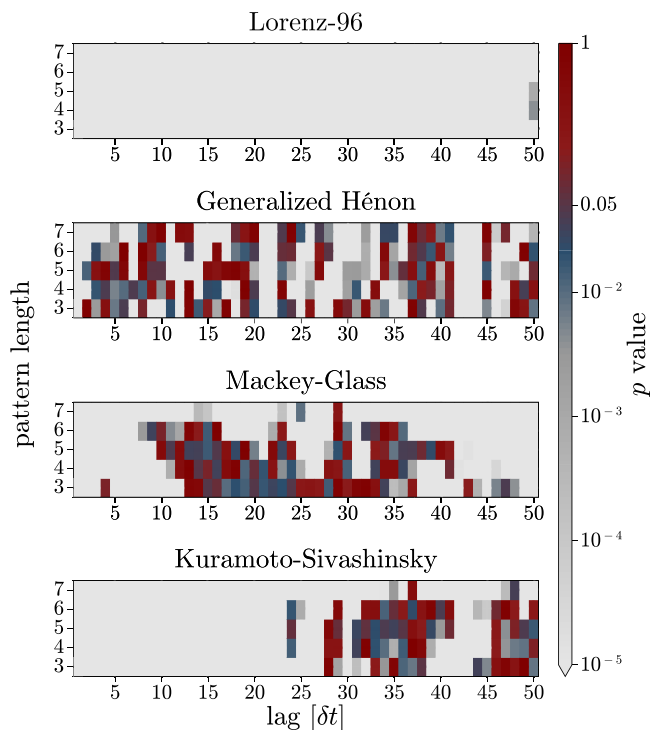


FIG. 5. Significance of an AAFT-surrogate data test across different pattern lengths m and lags l for the considered dynamical systems. Each system had a KY dimension of $\Delta^{(KY)} \approx 43$ (corresponding values for D , τ , and L are given in Table I), and time series with $N = 10^6$ points were considered. The p -value was calculated in a two-sample Kolmogorov–Smirnov test³⁵ with 50 FT surrogates each and one original time series. The corresponding plots for FT surrogates are shown in Fig. 8 of the Appendix.

measure enough data. For this estimation, we used the large amount of $N = 10^6$ data points.

B. Given parameters: Attractor dimensionality and the amount of data

In this study, we address the scientific question what happens with the CE-analysis if the time series of interest was generated by a deterministic system with a chaotic attractor of (unknown) high dimensionality. Therefore, we investigated the influence of the attractor dimensionality on the position of points in the CE plane as shown in Fig. 6. For a constant pattern length m and lag l , the position of a time series in the CE plane quickly moves to the lower right corner of the plane, where purely stochastic systems would be expected. It should be mentioned again that for the continuous-time systems, this depends significantly on the chosen lag l for a given sampling time δt . For very small sampling times and lags, even systems with $\Delta^{(KY)} \approx 43$ display a high complexity and low to intermediate permutation entropy, as can also be observed in Fig. 4. In this case, the high complexity values are mostly a result of the smoothness of the finely sampled smooth continuous time series, which leads by construction to some patterns appearing significantly

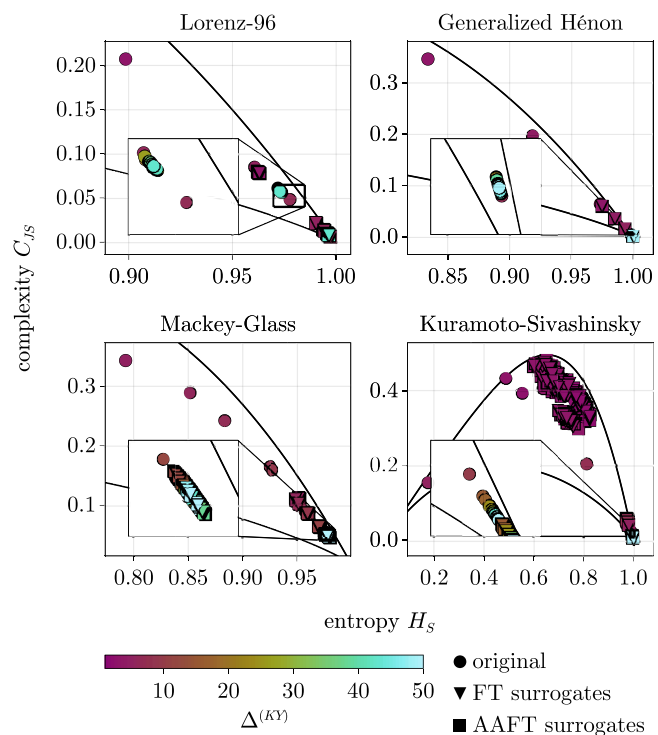


FIG. 6. Complexity–entropy values for time series from dynamics with different Kaplan–Yorke attractor dimensions. 10^6 points were considered with a pattern length of $m = 6$. The lags were fixed to $l = 10\delta t$ for the continuous-time systems and $l = 1$ for the generalized Hénon map. The solid black lines indicate the minimum and maximum possible complexity values for given entropy.

more often than others (e.g., strictly increasing or decreasing patterns). Again, in Fig. 4, there is almost no difference in CE values of FT- and AAFT-surrogate time series.

Figure 7 is an illustration of how statistical complexity and permutation entropy can be significantly over- and underestimated, respectively, if calculated from too little data. Both of these biases are expected due to the already discussed fact that the bins of the histograms must be properly filled.

Interestingly, the convergence to a limit appears to happen faster than one can naïvely expect when considering the amount of $m!$ possible ordinal patterns. This could be considered an indication of *forbidden patterns*^{66,67} in the here considered chaotic systems, meaning that there are much less truly possible ordinal patterns, and thus, a significantly smaller amount of data is needed to correctly estimate the ordinal probability distribution.

V. DISCUSSION

Previous work has shown that time series generated by low-dimensional dynamical systems can be distinguished from stochastic time series (noise) by means of their entropy and statistical complexity values, both computed using ordinal pattern statistics.⁴ In this work, we addressed the question, whether

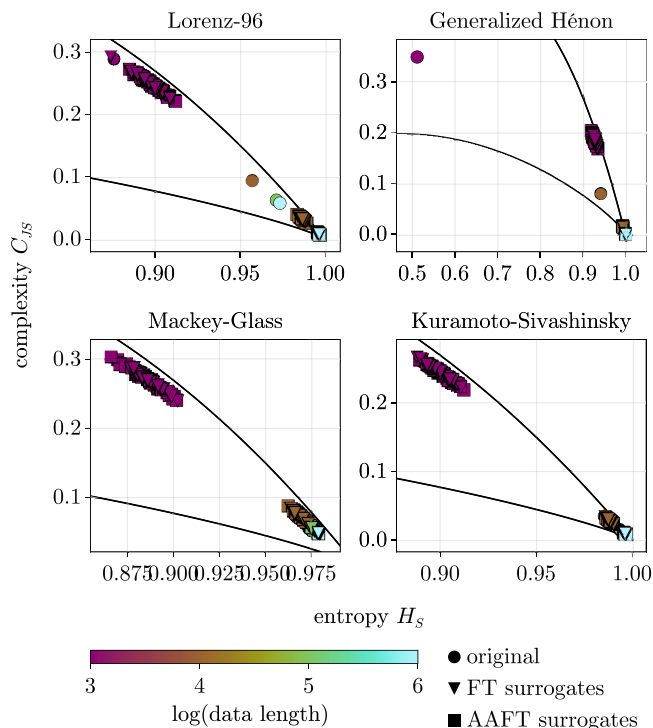


FIG. 7. Complexity–entropy values for patterns of different data lengths. Systems with $\Delta^{(KY)} \approx 43$ (corresponding values for D , τ , L are given in Table I) were considered with patterns of length $m = 6$. The lags were fixed to $l = 10\delta t$ for the continuous-time systems and $l = 1$ for the generalized Hénon map. The solid black lines indicate the minimum and maximum possible complexity values for given entropy.

this approach is also feasible with data from systems with high-dimensional chaotic attractors. As examples, we used time series from the Lorenz-96 system, a generalized Hénon map, the Mackey–Glass delay-differential equation, and the spatially extended Kuramoto–Sivashinsky equation given by a partial differential equation. For these systems, control parameters exist that allow one to increase the attractor dimension in a systematic manner that we used to generate data with Kaplan–Yorke dimensions ranging from 1 up to 50. The representation (i.e., location) of the time series in the complexity–entropy plane was studied, not only for varying attractor dimensions, but also its dependence on the length of the time series available and the length and lag of the ordinal patterns used. Furthermore, these results were compared with the corresponding values obtained for phase-randomized surrogate time series.

Both the entropy and the statistical complexity measure a deviation of the distribution of patterns to a uniform distribution, albeit in different ways. There are, however, at least two reasons why this deviation can be overestimated resulting in spuriously low entropies and spuriously high values of the statistical complexity. In the case of very densely sampled smooth continuous time series, (highly) nonuniform distributions of ordinal patterns occur even for stochastic data, obtained by phase randomization, for example. In this case,

any (complexity, entropy)-curve in the CE plane parameterized by the lag exhibits a local maximum of the complexity for intermediate pattern lags, and it had been suggested to focus at complexity values at this maximum for distinguishing chaotic and stochastic dynamics.¹² Our results show, however, that phase-randomized surrogate data follow the same path along the CE plane and have a very similar maximum. This limitation and the characteristic shape of the lag curve in the CE plane (Fig. 4) also occur with time series from low-dimensional chaotic systems (not shown here). Interestingly, amplitude adjusted phase-randomized (AAFT) and (just) phase-randomized (FT) surrogates provide essentially the same results because the adjustment has almost no impact on ordinal pattern distributions.

The second reason for observing (highly) non-uniform distributions is too few data points required for a sound estimation of ordinal pattern distributions. This problem occurs, in particular, for high dimensional time series. There, the pattern length has to exceed some lower bound to resolve or unfold the dynamics. Below this critical pattern length, the resulting distribution is close to a uniform distribution and not suitable for distinguishing the data from noise. If, however, the pattern length m is increased, the number of bins grow as $m!$ and the corresponding distribution has empty or poorly filled bins due to too few data points, even for long time series.

To avoid or at least detect both pitfalls resulting in spuriously low entropy and spuriously high complexity values, we suggest a comparison with the corresponding values of phase-randomized surrogate data because both reasons for highly nonuniform distributions have essentially the same effect for smooth stochastic data. If the null hypothesis that the given time series deviates from a linear stochastic process cannot be rejected using a combination of permutation entropy and statistical complexity as a discriminating statistic (see Sec. II A), any resulting position in the CE plane should be interpreted with caution. For this evaluation, diagrams, such as those shown in Figs. 3–5, provide valuable information, whether the desired characterization of the data using the location in the CE plane can be considered meaningful at all. Keeping in mind that for very high-dimensional data, large pattern lengths would be needed to properly separate chaos from noise, the often limited amount of data makes the estimation of such finely partitioned distributions difficult to impossible.

ACKNOWLEDGMENTS

We thank George Datsis, Stefan Luther, Alexander Schlemmer, and all members of the Research Group Biomedical Physics for continuous support and inspiring discussions and the reviewers for very constructive remarks. Furthermore, financial support by the German Centre for Cardiovascular Research (DZHK) e.V. and the Max Planck Society is gratefully acknowledged.

AUTHOR DECLARATIONS

Conflict of Interest

The authors have no conflicts to disclose.

Author Contributions

Inga Kottlarz: Conceptualization (supporting); Data curation (lead); Formal analysis (lead); Investigation (equal); Software (lead); Validation (equal); Visualization (lead); Writing – original draft (lead). **Ulrich Parlitz:** Conceptualization (lead); Investigation (equal); Project administration (lead); Supervision (lead); Validation (equal); Writing – review & editing (lead).

DATA AVAILABILITY

The code to produce the data that support the findings of this study are openly available in GitHub at <https://github.com/ikottlarz/HighDimensionalComplexityEntropy>.

APPENDIX: FT VS Aaft SURROGATES

Figure 8 shows the significance of an FT surrogate data test depending on (m, l) . It can be seen that the results are very similar to those shown in Fig. 5.

Figure 9 shows the distributions of the normalized permutation entropy for both Aaft and FT surrogates, once for each of the dynamical systems considered in this paper. We find that the

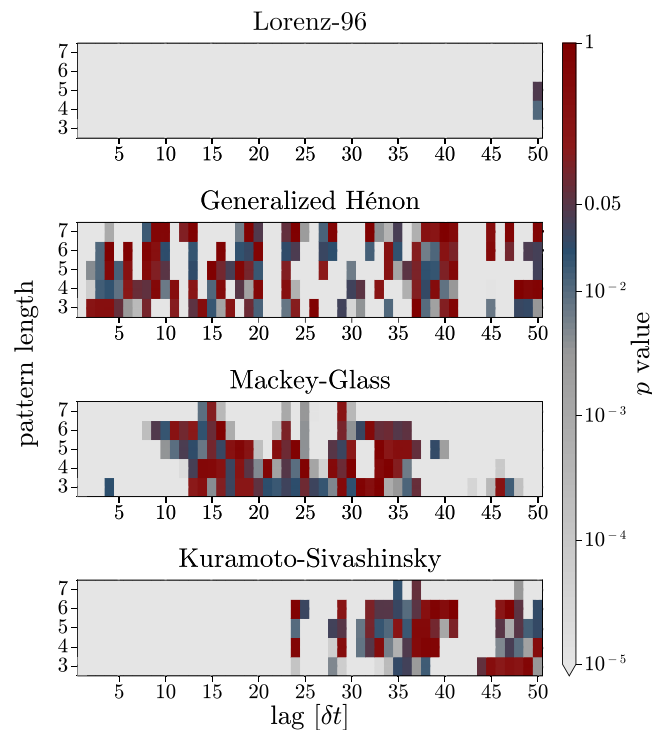


FIG. 8. Significance of an FT surrogate data test across different pattern lengths m and lags l for the considered dynamical systems. Each system had a KY dimension of $\Delta^{(KY)} \approx 43$ (corresponding values for D , τ , and L are given in Table I), and time series with $N = 10^6$ points were considered. The p -value was calculated in a two-sample Kolmogorov–Smirnov test³⁵ with 50 FT surrogates each and one original time series.

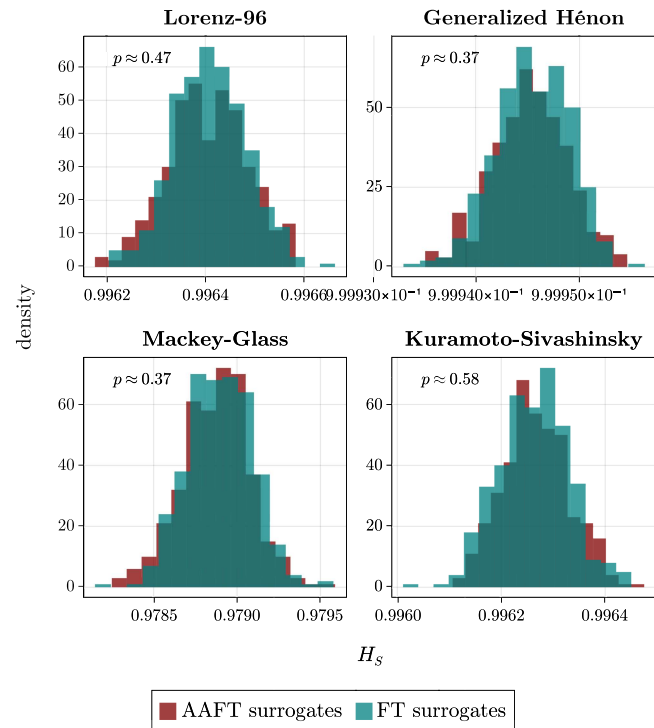


FIG. 9. Distributions of the normalized permutation entropy H_S ($m = 6, l = 10\delta t$ for the continuous-time systems and $l = 1$ for the generalized Hénon map) for 400 FT/Aaft surrogates each. The surrogates were generated from the time series of length $N = 10^6$ from systems with $\Delta^{(KY)} \approx 43$. The p -value was calculated in a two-sample Kolmogorov–Smirnov test³⁵ with 50 FT surrogates each and one original time series.

distributions of normalized permutation entropy of FT and Aaft surrogates are indistinguishable. Presumably, this is due to the fact that ordinal patterns are invariant with respect to monotonous amplitude transformations.

REFERENCES

1. P. Crutchfield and K. Young, “Inferring statistical complexity,” *Phys. Rev. Lett.* **63**, 105–108 (1989).
2. C. Adami, “What is complexity?,” *BioEssays* **24**, 1085–1094 (2002).
3. C. Bandt and B. Pompe, “Permutation entropy: A natural complexity measure for time series,” *Phys. Rev. Lett.* **88**, 174102 (2002).
4. O. A. Rosso, H. A. Larrondo, M. T. Martin, A. Plastino, and M. A. Fuentes, “Distinguishing noise from chaos,” *Phys. Rev. Lett.* **99**, 154102 (2007).
5. M. Small, “Complex networks from time series: Capturing dynamics,” in *2013 IEEE International Symposium on Circuits and Systems (ISCAS)* (IEEE, 2013), pp. 2509–2512, ISSN: 2158-1525.
6. A. A. B. Pessa and H. V. Ribeiro, “Characterizing stochastic time series with ordinal networks,” *Phys. Rev. E* **100**, 042304 (2019).
7. P. Grassberger, “Randomness, information, and complexity,” *arXiv:1208.3459v1* (2012).
8. J. M. Amigó, R. Dale, and P. Tempesta, “Permutation group entropy: A new route to complexity for real-valued processes,” *Chaos* **32**, 112101 (2022).
9. C. Tsitouras, “Runge–Kutta pairs of order 5(4) satisfying only the first column simplifying assumption,” *Comput. Math. Appl.* **62**, 770–775 (2011).

- ¹⁰H. V. Ribeiro, L. Zunino, R. S. Mendes, and E. K. Lenzi, “Complexity–entropy causality plane: A useful approach for distinguishing songs,” *Phys. A* **391**, 2421–2428 (2012).
- ¹¹H. V. Ribeiro, L. Zunino, E. K. Lenzi, P. A. Santoro, and R. S. Mendes, “Complexity–entropy causality plane as a complexity measure for two-dimensional patterns,” *PLoS One* **7**, e40689 (2012).
- ¹²L. Zunino, M. C. Soriano, and O. A. Rosso, “Distinguishing chaotic and stochastic dynamics from time series by using a multiscale symbolic approach,” *Phys. Rev. E* **86**, 046210 (2012).
- ¹³L. Zunino and H. V. Ribeiro, “Discriminating image textures with the multiscale two-dimensional complexity–entropy causality plane,” *Chaos, Solitons Fractals* **91**, 679–688 (2016).
- ¹⁴L. H. Fernandes and F. H. Araújo, “Taxonomy of commodities assets via complexity–entropy causality plane,” *Chaos, Solitons Fractals* **137**, 109909 (2020).
- ¹⁵J. L. Jara, C. Morales-Rojas, J. Fernández-Muñoz, V. J. Haunton, and M. Chacón, “Using complexity–entropy planes to detect Parkinson’s disease from short segments of haemodynamic signals,” *Physiol. Meas.* **42**, 084002 (2021).
- ¹⁶I. Leyva, J. H. Martínez, C. Masoller, O. A. Rosso, and M. Zanin, “20 years of ordinal patterns: Perspectives and challenges,” *Europhys. Lett.* **138**, 31001 (2022).
- ¹⁷P. Martínez Coq, A. Rey, O. A. Rosso, R. Armentano, and W. Legnani, “Detection of cardiac arrhythmia patterns in ECG through $H \times C$ plane,” *Chaos* **32**, 123118 (2022).
- ¹⁸I. Daniel de Carvalho Barreto, T. Stosic, R. S. Cezar Menezes, A. S. Alves da Silva, O. A. Rosso, and B. Stosic, “Hydrological changes caused by the construction of dams and reservoirs: The CECP analysis,” *Chaos* **33**, 023115 (2023).
- ¹⁹L. Glass and M. C. Mackey, “Pathological conditions resulting from instabilities in physiological control systems,” *Ann. N.Y. Acad. Sci.* **316**, 214–235 (1979).
- ²⁰E. Lorenz, “Predictability: A problem partly solved,” in *Seminar on Predictability, Shinfield Park, Reading, UK, 4–8 September 1995* (ECMWF, 1995), Vol. 1, pp. 1–18.
- ²¹G. Baier and M. Klein, “Maximum hyperchaos in generalized Hénon maps,” *Phys. Lett. A* **151**, 281–284 (1990).
- ²²J. Sprott, “High-dimensional dynamics in the delayed Hénon map,” *Electron. J. Theor. Phys.* **3**, 19–35 (2006).
- ²³S. Bilal and R. Ramaswamy, “The generalized time-delayed Hénon map: Bifurcations and dynamics,” *Int. J. Bifurcation Chaos* **23**, 1350045 (2013).
- ²⁴G. Sivashinsky, “Nonlinear analysis of hydrodynamic instability in laminar flames—I. Derivation of basic equations,” *Acta Astronaut.* **4**, 1177–1206 (1977).
- ²⁵Y. Kuramoto, “Diffusion-induced chaos in reaction systems,” *Prog. Theor. Phys. Suppl.* **64**, 346–367 (1978).
- ²⁶M. C. Mackey and L. Glass, “Oscillation and chaos in physiological control systems,” *Science* **197**, 287–289 (1977).
- ²⁷J. Doyno Farmer, “Chaotic attractors of an infinite-dimensional dynamical system,” *Phys. D* **4**, 366–393 (1982).
- ²⁸G. Datsis and U. Parlitz, *Nonlinear Dynamics—A Concise Introduction Interlaced with Code* (Springer, 2022).
- ²⁹G. Datsis, “DynamicalSystems.jl: A Julia software library for chaos and nonlinear dynamics,” *J. Open Source Softw.* **3**, 598 (2018).
- ³⁰G. Lancaster, D. Iatsenko, A. Pidde, V. Ticcinelli, and A. Stefanovska, “Surrogate data for hypothesis testing of physical systems,” *Phys. Rep.* **748**, 1–60 (2018).
- ³¹J. Theiler, S. Eubank, A. Longtin, B. Galdrikian, and J. Doyno Farmer, “Testing for nonlinearity in time series: The method of surrogate data,” *Phys. D* **58**, 77–94 (1992).
- ³²B. Efron, “Computers and the theory of statistics: Thinking the unthinkable,” *SIAM Rev.* **21**, 460–480 (1979).
- ³³N. Wiener, “Generalized harmonic analysis,” *Acta Math.* **55**, 117–258 (1930).
- ³⁴A. Khintchine, “Korrelationstheorie der stationären stochastischen prozesse,” *Math. Ann.* **109**, 604–615 (1934).
- ³⁵J. W. Pratt and J. D. Gibbons, “Kolmogorov–Smirnov two-sample tests,” in *Concepts of Nonparametric Theory*, Springer Series in Statistics, edited by J. W. Pratt and J. D. Gibbons (Springer, New York, 1981), pp. 318–344.
- ³⁶M. Morse and G. A. Hedlund, “Symbolic dynamics,” *Am. J. Math.* **60**, 815–866 (1938).
- ³⁷U. Parlitz *et al.*, “Classifying cardiac biosignals using ordinal pattern statistics and symbolic dynamics,” *Comput. Biol. Med.* **42**, 319–327 (2012).
- ³⁸A. M. Unakafov, “Ordinal-patterns-based segmentation and discrimination of time series with applications to EEG data,” Ph.D. thesis (University of Lübeck, 2015).
- ³⁹K. Keller *et al.*, “Ordinal patterns, entropy, and EEG,” *Entropy* **16**, 6212–6239 (2014).
- ⁴⁰G. Graff *et al.*, “Ordinal pattern statistics for the assessment of heart rate variability,” *Eur. Phys. J. Spec. Top.* **222**, 525 (2013).
- ⁴¹K. Keller, M. Sinn, and J. Emonds, “Time series from the ordinal viewpoint,” *Stoch. Dyn.* **07**, 247 (2007).
- ⁴²L. Waschke, M. Wöstmann, and J. Obleser, “States and traits of neural irregularity in the age-varying human brain,” *Sci. Rep.* **7**, 17381 (2017).
- ⁴³I. Kottlarz, S. Berg, D. Toscano-Tejeida, I. Steinmann, M. Bähr, S. Luther, M. Wilke, U. Parlitz, and A. Schlemmer, “Extracting robust biomarkers from multichannel EEG time series using nonlinear dimensionality reduction applied to ordinal pattern statistics and spectral quantities,” *Front. Physiol.* **11**, 614565 (2021).
- ⁴⁴K. Lehnertz, “Ordinal methods for a characterization of evolving functional brain networks,” *Chaos* **33**, 022101 (2023).
- ⁴⁵A. Bahraminasab, F. Ghasemi, A. Stefanovska, P. V. E. McClintock, and H. Kantz, “Direction of coupling from phases of interacting oscillators: A permutation information approach,” *Phys. Rev. Lett.* **100**, 084101 (2008).
- ⁴⁶I. Echevoyen, V. Vera-Ávila, R. Sevilla-Escoboza, J. H. Martínez, and J. M. Buldú, “Ordinal synchronization: Using ordinal patterns to capture interdependencies between time series,” *Chaos, Solitons Fractals* **119**, 8–18 (2019).
- ⁴⁷J. Zhang, J. Zhou, M. Tang, H. Guo, M. Small, and Y. Zou, “Constructing ordinal partition transition networks from multivariate time series,” *Sci. Rep.* **7**, 7795 (2017).
- ⁴⁸J. Tiana-Alsina, C. Quintero-Quiroz, M. C. Torrent, and C. Masoller, “Quantifying the degree of locking in weakly forced stochastic systems,” *Phys. Rev. E* **99**, 022207 (2019).
- ⁴⁹J. Tiana-Alsina, C. Quintero-Quiroz, and C. Masoller, “Comparing the dynamics of periodically forced lasers and neurons,” *New J. Phys.* **21**, 103039 (2019).
- ⁵⁰A. Aragonese, S. Perrone, T. Sorrentino, M. C. Torrent, and C. Masoller, “Unveiling the complex organization of recurrent patterns in spiking dynamical systems,” *Sci. Rep.* **4**, 4696 (2014).
- ⁵¹J. A. Reinoso, M. C. Torrent, and C. Masoller, “Emergence of spike correlations in periodically forced excitable systems,” *Phys. Rev. E* **94**, 032218 (2016).
- ⁵²K. A. Haaga, G. Datsis, I. Kottlarz, A. White, HeineRugland, and S. G. Johnson, “JuliaDynamics/ComplexityMeasures.jl: v2.7.1.”
- ⁵³C. E. Shannon, “A mathematical theory of communication,” *Bell Syst. Tech. J.* **27**, 379–423 (1948).
- ⁵⁴The permutation entropy is a feature of the given time series, not of the underlying dynamical system or process, because it depends on the observation or measurement function providing the data.
- ⁵⁵O. Rosso, M. Martin, H. Larrondo, A. Kowalski, and A. Plastino, “Generalized statistical complexity: A new tool for dynamical systems,” in *Concepts and Recent Advances in Generalized Information Measures and Statistics* (Bentham Science Publishers, 2013), pp. 169–215.
- ⁵⁶M. T. Martin, A. Plastino, and O. A. Rosso, “Generalized statistical complexity measures: Geometrical and analytical properties,” *Phys. A* **369**, 439–462 (2006).
- ⁵⁷Important: Here, we do not speak of the concept of patterns that are forbidden due to the underlying dynamics, but only due to the sampling!
- ⁵⁸J.-P. Eckmann and D. Ruelle, “Fundamental limitations for estimating dimensions and Lyapunov exponents in dynamical systems,” *Phys. D* **56**, 185–187 (1992).
- ⁵⁹L. A. Smith, “Intrinsic limits on dimension calculations,” *Phys. Lett. A* **133**, 283–288 (1988).
- ⁶⁰E. J. Kostelich and H. L. Swinney, “Practical considerations in estimating dimension from time series data,” *Phys. Scr.* **40**, 436 (1989).

⁶¹D. Ruelle, Proc. R. Soc. Lond. A **427**, 241 (1990).

⁶²H. Whitney, "Differentiable manifolds," *Ann. Math.* **37**, 645–680 (1936).

⁶³F. Takens, "Detecting strange attractors in turbulence," in *Dynamical Systems and Turbulence, Warwick 1980*, Lecture Notes in Mathematics, edited by D. Rand and L.-S. Young (Springer, 1981), pp. 366–381.

⁶⁴T. Sauer, J. A. Yorke, and M. Casdagli, "Embedology," *J. Stat. Phys.* **65**, 579–616 (1991).

⁶⁵For example, for $m = 2$, the ordinal pattern distribution of a period sinusoidal signal is uniform.

⁶⁶J. M. Amigó, S. Zambrano, and M. A. F. Sanjuán, "True and false forbidden patterns in deterministic and random dynamics," *Europhys. Lett.* **79**, 50001 (2007).

⁶⁷O. A. Rosso, L. C. Carpi, P. M. Saco, M. G. Ravetti, H. A. Larrondo, and A. Plastino, "The Amigó paradigm of forbidden/missing patterns: A detailed analysis," *Eur. Phys. J. B* **85**, 419 (2012).

⁶⁸L. Zunino, F. Olivares, F. Scholkmann, and O. A. Rosso, "Permutation entropy based time series analysis: Equalities in the input signal can lead to false conclusions," *Phys. Lett. A* **381**(22), 1883–1892 (2017).